united nations
educational, scientific
and cultural
organization

international atomic
energy agency

the
abdus salam
international centre for theoretical physics

SMR 1302 - 7

WINTER SCHOOL ON LASER SPECTROSCOPY AND APPLICATIONS

19 February - 2 March 2001

LASER OPTOGALVANIC SPECTROSCOPY OF INERT GASES

M. Aslam BAIG
Atomic and Molecular Physics Laboratory
Quaid-i-Azam University, Islamabad, Pakistan

Laser Optogalvanic Spectroscopy of inert gases

M. Aslam Baig
Atomic and Molecular Physics Laboratory
Quaid-i-Azam University, Islamabad, Pakistan

- Basic Process
- Experimental arrangements
- Single photon excitation
- Double resonance experiments
- Bound states
- Autoionizing resonances
- Data interpretation

EXPERIMENTAL ARRANGEMENT

Excitation sources:

CW Lasers
Pulsed Lasers

Detection Systems:

Hollow Cathode lamps
Discharge Cells

Typical Experimental Setup:

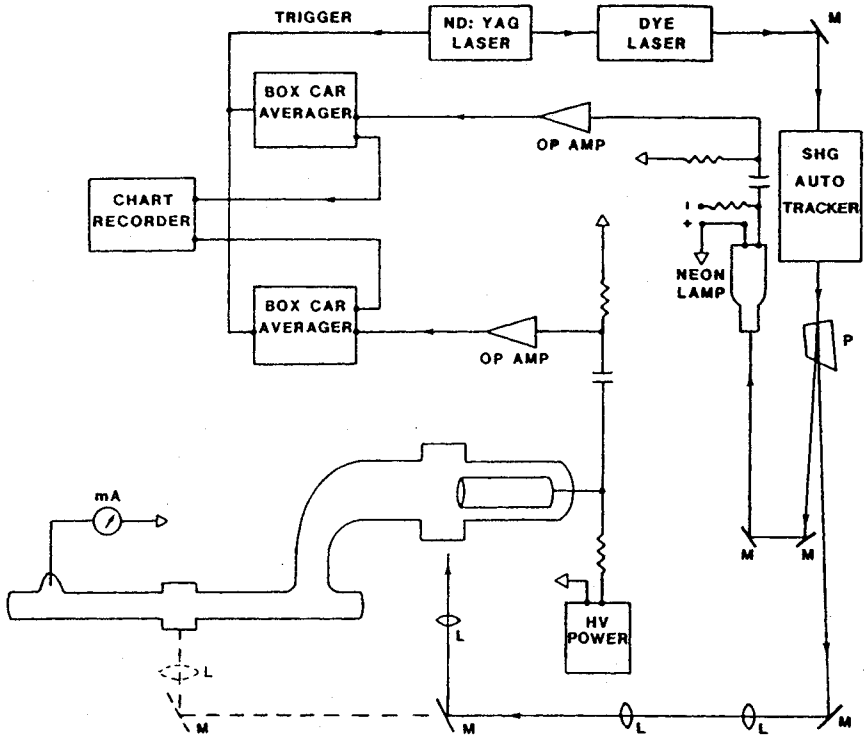

2. The Spectrum of helium:

The ground state electronic configuration of helium is $1s^2\ ^1S_0$. The $2s\ ^3S$ metastable level at 159856.069 cm^{-1} lies lower in energy than the metastable $2s\ ^1S$ level at 166277.546 cm^{-1}. In a discharge, the metastable levels are highly populated and the laser excitations from these levels result in strong optogalvanic signals.

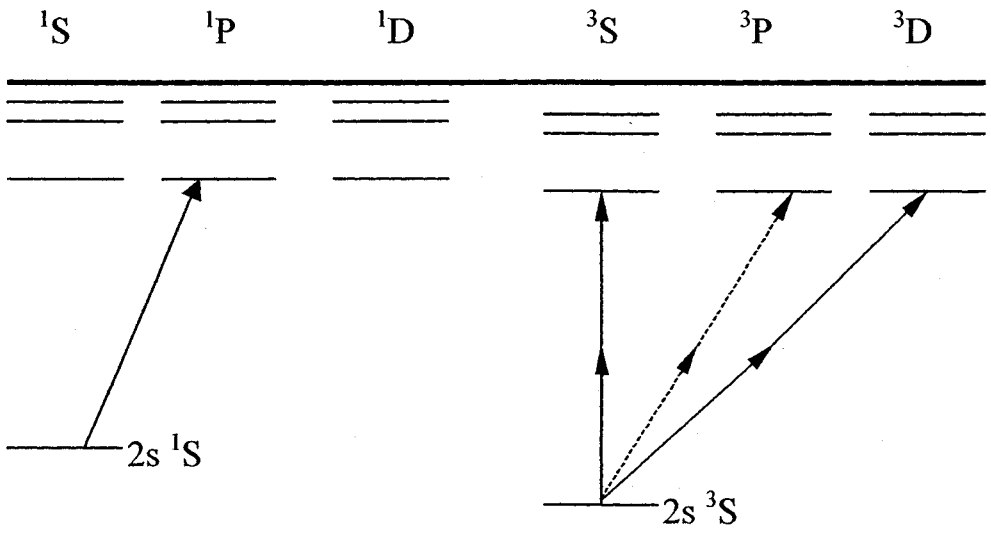

Energy level diagram of helium

Katayama et al (1979) used a discharge cell to record the one-photon excitation spectrum of helium using a frequency doubled out put of a pulsed dye laser in the spectral region covering $n = 14$ to $n = 36$. It was noticed that the lines are not shifted and the widths of the lines are also corresponding to the width of the laser 0.5 cm^{-1}.

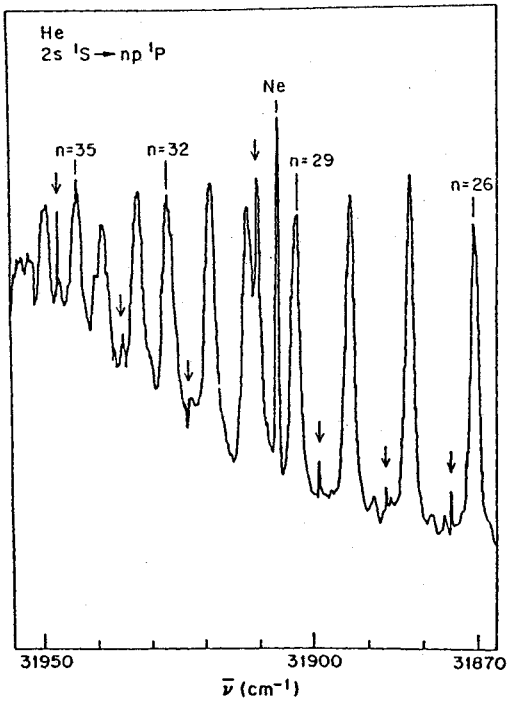

Panock et al (1980) investigated the highly excited states of helium using multiphoton excitation and subsequent ionization detection technique. The 2s $^3S \rightarrow np\ ^3P$ series ($16 \leq n \leq 37$) were recorded by the single photon excitation, laser excitation wavelength 260.5 – 263.0 nm whereas, the intervals between the $ns\ ^3S$– $nd\ ^3D$ levels were measured for ($16 \leq n \leq 22$).

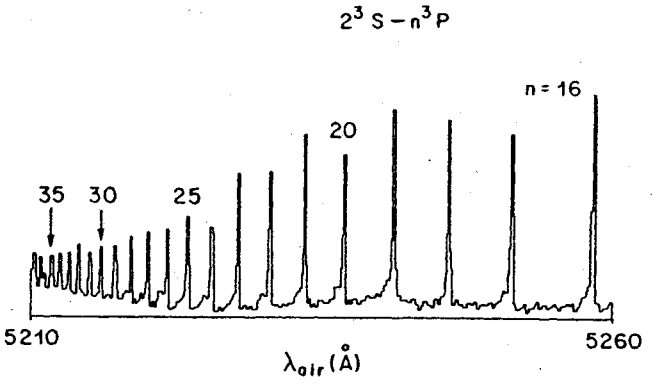

Ganguly (1986) measured the high Rydberg spectra of atomic helium, $np\ ^1P$ series up to $n = 46$ in the negative glow region of a discharge using $m_j = \pm 1$ polarization.

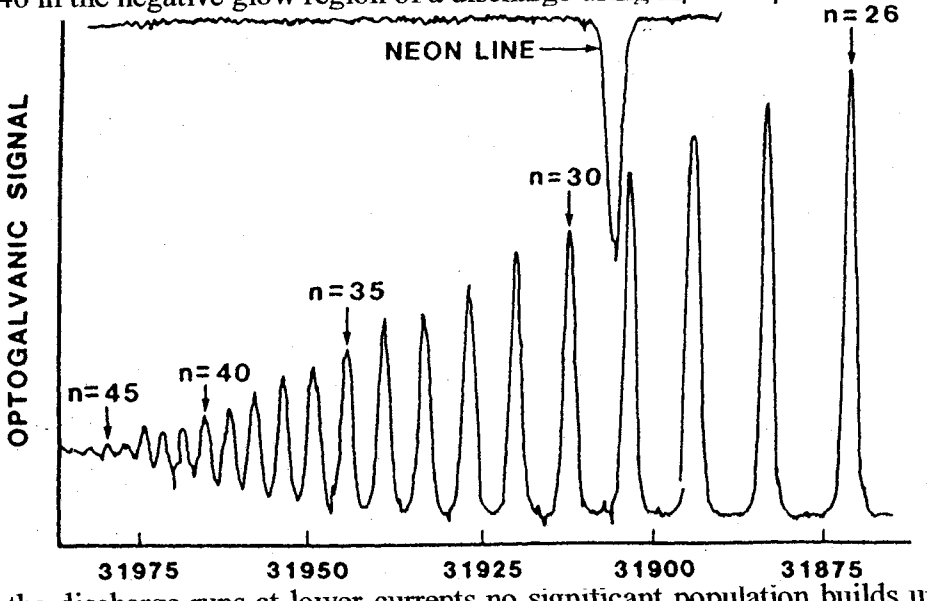

When the discharge runs at lower currents no significant population builds up in the higher energy levels. By scanning the laser, we have recorded the spectra that appear as a result of two-photon excitation from the 2s ^3S and the 2s ^1S metastable levels.

In a two-photon excitation, the strength of a transition is proportional to the square of the radiation intensity. For a Gaussian beam, a tightly focused laser can probe the discharge with better resolution. This means that the two-photon signal will build up

only in the close vicinity of the laser beam waist. The electric field, manifested through the spectra, can therefore be explored using a focused beam propagating axially through the discharge cell. The laser beam was focussed at several positions between the two electrodes and studied the triplet helium spectrum by two-photon excitation from the 2s ^{3}S metastable level. A set of spectra around 17d ^{3}D is measured at various spatial locations between the two electrodes is shown below. When the laser is focused close to the cathode, three lines 17s ^{3}S, 17p ^{3}P and 7d ^{3}D have been observed, the 17d ^{3}D line being the most intense. As the focussed laser beam is moved towards the anode, the intensity of this line first increases reaches to a maximum near the middle of the inter-electrode spacing and then starts decreasing.

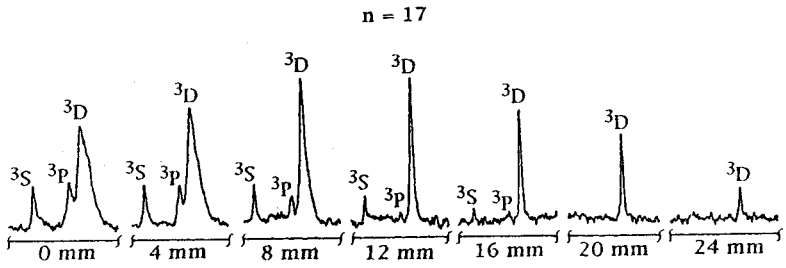

The spectra of helium for n=7 recorded at varying distances from the cathode.

The widths of the 17d ^{3}D line show a systematic decrease all the way from cathode to anode. The full width at half maximum (FWHM) of the 17d ^{3}D line close to anode is $\cong$ 0.4 cm^{-1} which becomes $\cong$ 2.0 cm^{-1} near the cathode. Another significant feature of the 17d ^{3}D line is its energy shift which starts increasing from anode to cathode. No observable shift has been detected in the line recorded near the anode, whereas, near the cathode the line is shifted to $\cong$ 0.6 cm^{-1}. The estimated electric field in the region close to cathode is $\cong$30V/cm, based on the observed FWHM and shift of the line. The field near the anode is quite small and does not express itself for this *n* value. The higher field near the cathode has caused Stark mixing of the levels which is manifested by the appearance of the two-photon parity forbidden 2s ^{3}S to 17p ^{3}P transition. The relative intensity of the17p ^{3}P line, therefore, decreases with the distance away from the cathode.

The optogalvanic spectra of helium in the region from 521 - 536 nm at locations near the anode and the cathode are shown below. It provides field free spectrum near the anode in contrast to that near the cathode where the field effects (shifts and ℓ-mixing

etc.) is clearly enhanced. The observed two-photon transitions are assigned as Rydberg series

$$2s\,^3S \rightarrow n\mathrm{d}\,^3D$$
$$\rightarrow n\mathrm{s}\,^3S$$
$$\rightarrow n\mathrm{s}\,^3P.$$

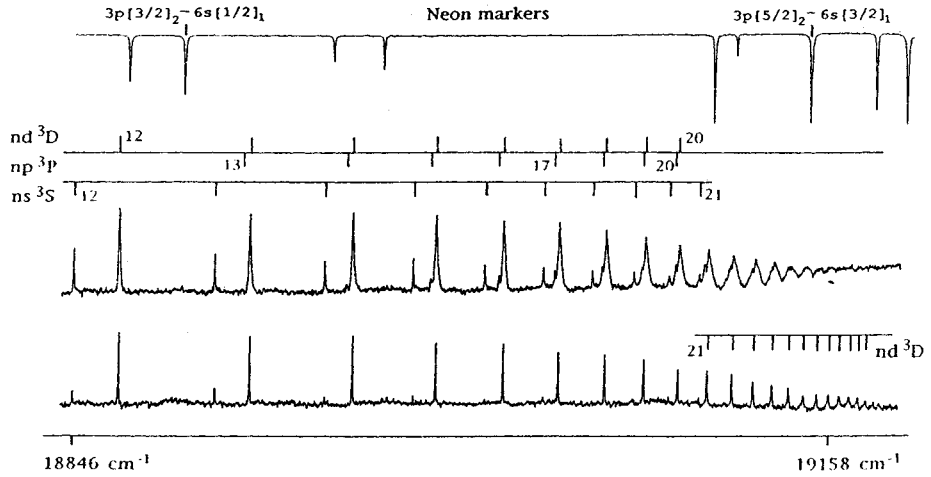

Fig. 3.1 *The Rydberg spectra of helium near the cathode and near the anode.*

The spectrum of the first figure mainly corresponds to the $2s\,^3S \rightarrow n\mathrm{d}\,^3D$ transitions; the $n\mathrm{d}\,^3D$ levels are resolved up to $n = 35$. The $n\mathrm{s}\,^3S$ series on the other hand is much weaker and only a few lower members could be recorded. In the second figure, the $n\mathrm{d}\,^3D$ series members are observed for $n \leq 28$ and the $n\mathrm{s}\,^3S$ series members for $n \leq 22$. Another Rydberg series that appears in this spectrum corresponds to the two-photon parity forbidden $2s\,^3S \rightarrow n\mathrm{d}\,^3P$ transition. This series begins to emerge on the lower energy side of the $n\mathrm{d}\,^3D$ ($13 \leq n \leq 25$) series.

3. The spectra of neon:

A single photon excitation from the ground state yields five dipole allowed Rydberg series converging on to two limits. Three series namely $2p^5(^2P_{3/2})n\mathrm{d}\,[1/2]_1$, $n\mathrm{d}[3/2]_1$ and $n\mathrm{s}[3/2]_1$ are attached to the first ionization threshold and two series are attached to the second ionization threshold, $2p^5(^2P_{1/2})n\mathrm{d}\,[3/2]_1$ and $n\mathrm{s}[1/2]_1$. The lower members of the series built on the $2p^5(^2P_{1/2})$ ionic level play an interesting role: below the first ionization threshold they interact with the series possessing same K and J values resulting in series perturbations and above the first ionization threshold they decay into the $2p^5(^2P_{3/2})\varepsilon\ell$ adjacent continua and show Fano-type autoionizing line shapes (Fano 1960).

In order to study the optogalvanic spectra of neon, the metastable levels built on the $2p^5 3s$ configuration namely $2p^5 3s\ [1/2]_0$ and $[3/2]_2$ play a major role. However a single photon excitation from these level needs ultraviolet laser. However, this region can be studied using two-photon excitation technique. Since the two photon spectra from the J = 2 lower level will yield all the possible excited levels possessing J = 0,1,2 and 3, the observed spectra is very complicated. An alternate way is the selective excitation and ionization. That means, first populating the metastabel level via discharge, preparing the atoms in an intermediate level of particular K and J values and finally scanning the second laser to look for the high Rydberg levels. In neon, the more interesting and relevant intermediate level are based on $2p^5 3p'$ configuration as listed by Kaufman and Minnhagen (1972).

$2p^5 3p'\ [1/2]_1 = 151038.4524\ cm^{-1}$

$2p^5 3p'\ [3/2]_1 = 150772.1118\ cm^{-1}$

$2p^5 3p'\ [3/2]_2 = 150858.5079\ cm^{-1}$

The optogalvanic spectra of neon excited from the $2p^5 3p'\ [1/2]_1$, $[3/2]_1$ and $[3/2]_2$ intermediate levels covering the energy region 173550 – 173725 cm^{-1} are shown in Fig.3.2abc.

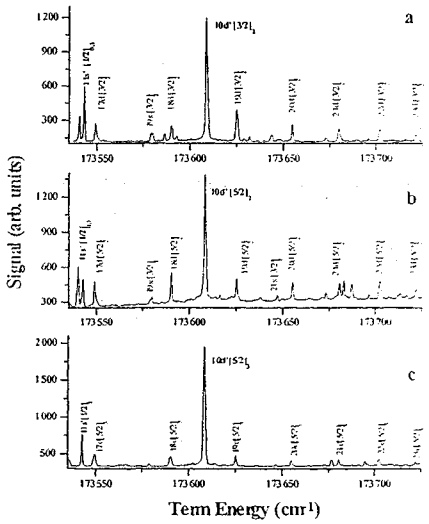

Figure 3.2 *The discrete structure in the perturbed region: (a) the discrete structure showing the $2p^5(^2P_{1/2})nd[3/2]_2$ series and $2p^5(^2P_{1/2})10d[3/2]_2$ interloper excited from the $2p^5(^2P_{1/2})3p[3/2]_1$ intermediate level. (b) the discrete structure showing the $2p^5(^2P_{1/2})nd[3/2]_2$ series and $2p^5(^2P_{1/2})10d[5/2]_2$ interloper excited from the $2p^5(^2P_{1/2})3p[3/2]_1$ intermediate level. (c) the discrete structure showing the $2p^5(^2P_{3/2})nd[5/2]_3$ series and $2p^5(^2P_{3/2})10d[5/2]_3$ interloper excited from the $2p^5(^2P_{3/2})3p[3/2]_2$ intermediate level.*

This region is selected because one of the lowest members of the *n*d and *n*s series that serve as perturbers lie in this region namely: $2p^5 10d'\ [3/2]_2$, $2p^5 10d'\ [5/2]_2$ and $2p^5 10d'\ [5/2]_3$ and $2p^5 11s'\ [1/2]_{0,1}$. In figure 3.2a the most intense lines are the perturber $2p^5 10d'\ [3/2]_2$ and $2p^5 11s'\ [1/2]_{0,1}$ and the prominent Rydberg attached to the first ionization limit are $nd[3/2]_2$ ($17 \leq n \leq 23$) and $ns[3/2]_2$ ($19 \leq n \leq 24$). In figure 3.2b the dominant line is $2p^5 10d'\ [5/2]_2$ and the two s-lines $2p^5 11s'\ [1/2]$ J = 1 and 0 possess similar intensities and the Rydberg attached to the first ionization limit are $nd[5/2]_2$ ($17 \leq n \leq 23$) and $ns[3/2]_1$ ($18 \leq n \leq 24$). The most strongest line in figure 3.2c is $2p^5 10d'\ [5/2]_3$ and the $2p^5 11s'\ [1/2]$ J = 0 is absent, in accordance to the selection rules in the $J_c\ell K$-coupling. The Rydberg attached to the first ionization limit are $nd[5/2]_3$ ($17 \leq n \leq 23$) and $ns[3/2]_2$ ($18 \leq n \leq 24$). In the present experiment we have been able to excite three different Rydberg series of definite K and J values from each of the three intermediate levels and the corresponding inter-channel interactions have been studied below and above the first ionization threshold. The propensity rules for electric dipole transitions in the $j\ell K$-coupling scheme are: $\Delta\ell = \pm 1$; $\Delta j = 0$; $\Delta K = 0, \pm 1$ and $\Delta J = 0, \pm 1$. It is worth mentioning that these rules are well behaved and wherever $\Delta K = \Delta J = +\Delta\ell$, the line possesses higher intensity. However, the $\Delta j = 0$ rule is not followed strictly since transitions with the change of the ionic core are also observed. Consequently, the Rydberg series built on $2p^5(^2P_{3/2})$ and $2p^5(^2P_{1/2})$ ionic levels have been observed with reasonable intensities. The following, relatively stronger, Rydberg series have been detected from each of the intermediate level converging to the $2p^5(^2P_{3/2})$ and $2p^5\ (^2P_{1/2})$ limits:

(a) $2p^5(^2P_{1/2})3p[1/2]_1 \rightarrow 2p^5(^2P_{3/2})\ nd\ [3/2]_2$
$(^2P_{1/2})\ nd\ [3/2]_2$

(b) $2p^5(^2P_{1/2})3p[3/2]_1 \rightarrow 2p^5(^2P_{3/2})\ nd\ [5/2]_2$
$(^2P_{1/2})\ nd\ [5/2]_2$

(c) $2p^5(^2P_{1/2})3p[3/2]_2 \rightarrow 2p^5(^2P_{3/2})\ nd\ [5/2]_3$
$(^2P_{1/2})\ nd\ [5/2]_3$

The other series such as $2p^5(^2P_{3/2,1/2})ns$ have also been observed, but with very weak intensity in the discrete region and quite strong in the autoionizing region.

The Rydberg series excited from the $2p^5 3p'\ [1/2]_1$, $[3/2]_1$ and $[3/2]_2$ intermediate levels showing the higher members of the series are reproduced in figures 3.3abc

respectively. The members of the series converging to the second ionization threshold namely nd' $[3/2]_2$ (n = 11 and 12) and ns' $[1/2]_{0,1}$ (n = 12 and 13) are much stronger than the Rydberg series nd$[3/2]_2$ and ns$[3/2]_2$ converging to the first ionization threshold. This is in accordance to the jK-coupling selection rules. Here $\Delta j_c = 0$ for the transitions attached to the second ionization threshold whereas, $\Delta j_c = 1$ for the transitions built on the first ionization limit. The energy position of the series limit are also marked in the figures.

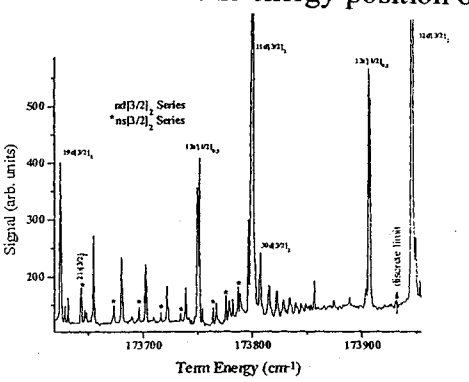

Figure 3.3a *Two-step laser optogalvanic spectra of neon covering the spectral region between 173620 – 173950 cm^{-1} excited from the $2p^5(^2P_{1/2})3p[1/2]_1$ intermediate level and converging to the first ionization limit.*

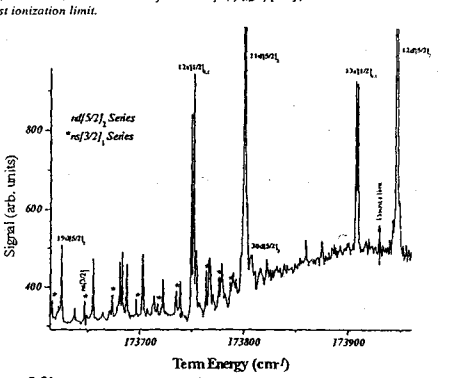

Figure 3.3b *Two-step laser optogalvanic spectra of neon covering the spectral region between 173620 – 173950 cm^{-1} excited from the $2p^5(^2P_{1/2})3p[3/2]_1$ intermediate level and converging to the first ionization limit.*

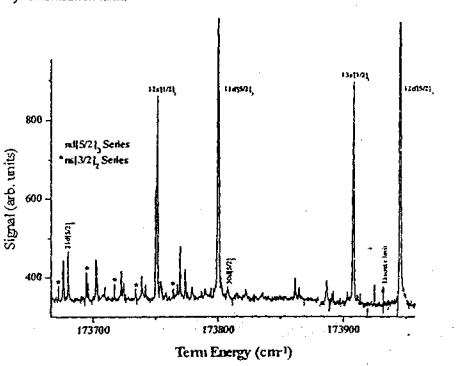

Figure 3.3c *Two-step laser optogalvanic spectra of neon covering the spectral region between 173620 – 173950 cm^{-1} excited from the $2p^5(^2P_{1/2})3p[3/2]_2$ intermediate level and converging to the first ionization limit.*

Fig. 3.3

The nd$[3/2]_2$ series have been observed up to n = 40 and the ns$[3/2]_1$ series up to n = 31. The 11d' $[3/2]_2$, 12s' $[1/2]_{0,1}$ and 13s' $[1/2]_{0,1}$ levels lies below the first ionization whereas, the 12d' $[3/2]_2$ level lies above the first ionization threshold. The Rydberg series excited from the $2p^5$3p' $[3/2]_1$ intermediate level is shown in figure 3.3b. In this

case the series attached to the first ionization threshold are nd[5/2]$_2$ and ns [3/2]$_1$ whereas the members of the Rydberg series to the second ionization limit are 11-12 d' [5/2]$_2$, and 12 – 13 s' [1/2]$_{0,1}$. The nd[5/2]$_2$ series have been observed up to n = 32 and the ns[3/2]$_1$ series up to n = 29. The Rydberg series excited from the $2p^5 3p'$ [3/2]$_2$ intermediate level is shown in figure 3.3c. In this case the series attached to the first ionization threshold are nd[5/2]$_3$ and ns [3/2]$_2$ whereas the members of the Rydberg series to the second ionization limit are 11-12 d' [5/2]$_3$, and 12 – 13 s' [1/2]$_1$. The nd[5/2]$_3$ series have been observed up to n = 34 and the ns[3/2]$_2$ series up to n = 31. It is noticed that the 29d J = 2, 3 overlap in energy with the 11d' J = 2, 3 levels in all the excitation schemes. The widths of the levels lying below and above the first ionization threshold remain essentially the same that indicate that these levels are not strongly coupled with the $2p(^2P_{3/2})\varepsilon\ell$ continuum. The widths of the autoionizing resonances can also be predicted from the analysis of the series perturbations in the discrete region.

4. Spectra of Argon:

The odd parity Rydberg levels of argon using two-step laser excitation from the $3p^5 4s[3/2]_2$ metastable level are presented here. Three intermediate levels pertaining to the $3p^5 4p$ configuration have been used to excite a particular Rydberg series of definite K and J quantum number attached to the $3p^5(^2P_{3/2})$ limit as well as to the $3p^5(^2P_{1/2})$ ionic level. The optogalvanic spectra of argon excited from the $3p^5 4p'$ [1/2]$_1$, [3/2]$_1$ and [3/2]$_2$ intermediate levels covering the energy region 126050 – 126225 cm^{-1} are shown in Fig.4.2abc. This region is selected because the lowest members of the nd and ns series that serve as perturbers lie in this region namely: $3p^5 7d'$ [3/2]$_2$, $3p^5 7d'$ [5/2]$_2$ and $3p^5 7d'$ [5/2]$_3$ and $3p^5 9s'$ [1/2]$_{0,1}$. In figure 4.2a the most intense lines are the perturber $3p^5 7d'$ [3/2]$_2$ and $3p^5 9s'$ [1/2]$_1$, in figure 4.2b the dominant line is $3p^5 7d'$ [5/2]$_2$ and the two s-lines $3p^5 9s'$ [1/2] J = 1 and 0 possess similar intensities whereas, the most strongest line in figure 4.2c is $3p^5 7d'$ [5/2]$_3$ and the $3p^5 9s'$ [1/2] J = 0 is absent, in accordance to the selection rules in the $J_c\ell$K-coupling. In the present experiment we have been able to excite three different Rydberg series of definite K and J values from each of the three intermediate levels and the corresponding inter-channel interactions have been studied below and above the first ionization threshold. The propensity rules for electric dipole transitions in the jℓK-coupling scheme are: $\Delta\ell = \pm 1$; $\Delta j = 0$; $\Delta K = 0, \pm 1$ and $\Delta J = 0, \pm 1$. It is worth

mentioning that these rules are well behaved and wherever $\Delta K = \Delta J = +\Delta\ell$, the line possesses higher intensity. However, the $\Delta j = 0$ rule is not followed strictly since transitions with the change of the ionic core are also observed. Consequently, the Rydberg series built on $3p^5(^2P_{3/2})$ and $3p^5(^2P_{1/2})$ ionic levels have been observed with reasonable intensities. The following, relatively stronger, Rydberg series have been detected from each of the intermediate level converging to the $3p^5(^2P_{3/2})$ and $3p^5$ $(^2P_{1/2})$ limits:

(a) $3p^5(^2P_{1/2})4p[1/2]_1 \rightarrow 3p^5(^2P_{3/2})\,n\text{d}\,[3/2]_2$
$(^2P_{1/2})\,n\text{d}\,[3/2]_2$

(b) $3p^5(^2P_{1/2})4p[3/2]_1 \rightarrow 3p^5(^2P_{3/2})\,n\text{d}\,[5/2]_2$
$(^2P_{1/2})\,n\text{d}\,[5/2]_2$

(c) $3p^5(^2P_{1/2})4p[3/2]_2 \rightarrow 3p^5(^2P_{3/2})\,n\text{d}\,[5/2]_3$
$(^2P_{1/2})\,n\text{d}\,[5/2]_3$

The other series such as $3p^5(^2P_{3/2,1/2})ns$ have also been observed, but with very weak intensity in the discrete region and quite strong in the autoionizing region.

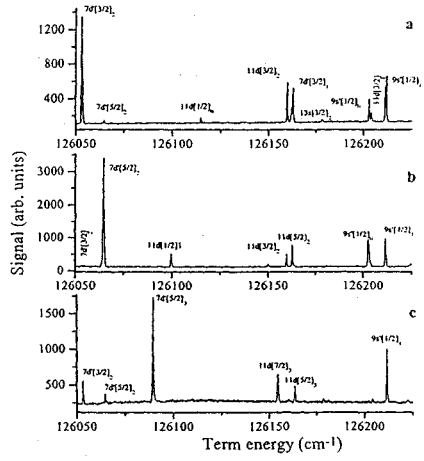

Figure 4.2 *Two-step laser optogalvanic spectra of argon covering the spectral region between 126050 cm^{-1} to 126225 cm^{-1} excited from (a) $3p^5(^2P_{1/2})4p[1/2]_1$ intermediate level (b) $3p^5(^2P_{1/2})4p[3/2]_1$ intermediate level (c) $3p^5(^2P_{1/2})4p[3/2]_2$ intermediate level.*

Fig. 4.2

The optogalvanic spectra of argon covering the energy region 126575 – 126800 cm^{-1} are shown in Fig.4.3abc. The $3p^5 8d'\ [3/2]_2$, $3p^5 8d'\ [5/2]_2$ and $3p^5 8d'\ [5/2]_3$ perturbers lie in this region revealing interesting intensity variations in the Rydberg series attached to the $3p^5(^2P_{3/2})$ ionization threshold. In Fig.4.3a the dominating line is $3p^5 8d'\ [3/2]_2$ along with the $3p^5(^2P_{3/2})nd\ [3/2]_2$ series. The $3p^5 16d\ [3/2]_2$ and $3p^5 17d\ [3/2]_2$ also appear with a comparable intensity. In Fig.4.3b the strongest line is $3p^5 8d'\ [5/2]_2$ and the nearby line $3p^5 16d\ [5/2]_2$ is also very prominent. The other members of the $3p^5 nd\ [3/2]_2$ series are very weak. In Fig.1c the $3p^5 8d'\ [5/2]_3$ line stands out clearly in addition to the $3p^5 nd\ [5/2]_3$ Rydberg series. Although the $3p^5(^2P_{3/2})nd\ [7/2]_3$ Rydberg series should have been present, it is too weak to be detected in this region. Weber et al (1999) have observed this series and remarked that this series possess almost constant quantum defect, show no significant perturbation, attributed to the fact that there does not exist any perturbing level possessing K = 7/2 and J = 3.

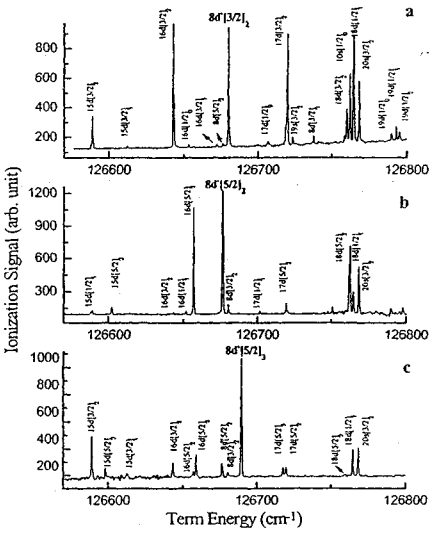

Figure 4.3 *The discrete structure in the perturbed region: (a) the discrete structure showing the $3p^5(^2P_{3/2})nd[3/2]_2$ series and $3p^5(^2P_{1/2})8d[3/2]_2$ interloper excited from the $3p^5(^2P_{1/2})4p[1/2]_1$ intermediate level; (b) the discrete structure showing the $3p^5(^2P_{3/2})nd[5/2]_2$ series and $3p^5(^2P_{1/2})8d[5/2]_2$ interloper excited from the $3p^5(^2P_{1/2})4p[3/2]_1$ intermediate level; (c) the discrete structure showing the $3p^5(^2P_{3/2})nd[5/2]_3$ series and $3p^5(^2P_{1/2})8d[5/2]_3$ interloper excited from the $3p^5(^2P_{1/2})4p[3/2]_2$ intermediate level.*

Fig. 4.3

The dominating intensities of the perturbers in this energy region clearly support their identifications as the lower members of the series built on the $3p^5(^2P_{1/2})$ ionic level. In particular, the relative intensities of the three perturbing levels alter as selecting different intermediate levels changes their excitation path. In Fig.4.3a, in addition to the $3p^5 8d'\ [3/2]_2$ line ($\Delta K = \Delta J = +\ell$) the $3p^5 8d'\ [5/2]_2$ line also appears, but with very small intensity. The relative low intensity of this line is in accord with the ΔK selection rule ($\Delta K = 2$ and $\Delta J = +\ell$). In Fig. 1b, the strongest line $3p^5 8d'\ [5/2]_2$ obey ($\Delta K = \Delta J = +\ell$) and the weak line $3p^5 8d'\ [3/2]_2$ ($\Delta K = 0$ and $\Delta J = +1$). However, all the three perturbers are visible in Fig.4.3c. The strongest line is $3p^5 8d'\ [5/2]_3$ ($\Delta K = \Delta J = +\ell$), the $3p^5 8d'\ [5/2]_2$ line is almost ten times weaker as compared to the strong line follows ($\Delta K = 1$ and $\Delta J = 0$) and the weakest line is $3p^5 8d'\ [3/2]_2$ according to ($\Delta K = 0$ and $\Delta J = 0$). The calculations of the relative intensities of the above mentioned lines (perturbers) by Faust and McFarlane (1968) indicate that the most probable transitions obey $\Delta K = \Delta J = +\ell$ selection rules and indeed it is in accordance with the present experimental results (see Fig. 4.3abc).

Figure 4.4 shows the spectrum of argon in the laser photon energy region 19293 - 19650 cm^{-1} observed by scanning the second laser while the first laser was tuned to the $3p^5 4p[1/2]_1$ intermediate level at 107496.461 cm^{-1} (Minhaggen 1973). The top spectrum is the optogalvanic spectrum from the hallow cathode that serves as the reference wavelength, the middle spectrum is the fringes from a 1mm thick solid etalon and the lower spectrum is the optogalvanic signal from the argon discharge cell.

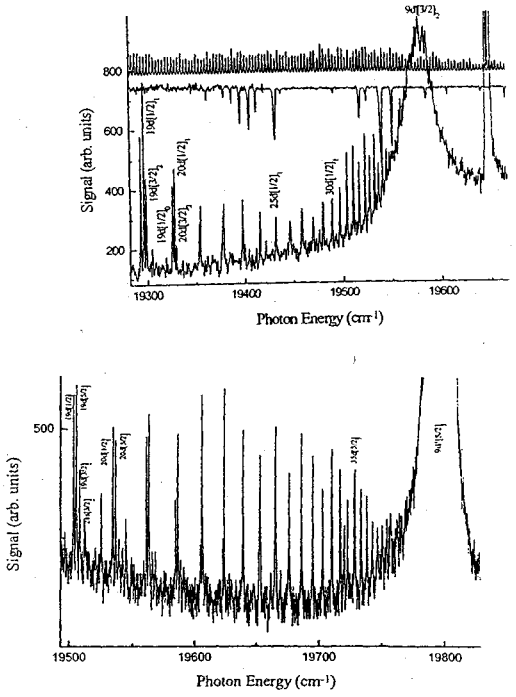

Fig. 4.4

The spectrum shows clearly two well established Rydberg series converging to the first ionization threshold. Faust and McFarlane (1968) reported the line strengths calculations for the p - d transitions. Accordingly, from the $3p^5 4p'\ [1/2]_1$ intermediate level the most probable upper level is $3p^5\ (^2P_{3/2})nd\ [3/2]_2$ carrying intensity 125, whereas, the $3p^5\ (^2P_{3/2})nd\ [1/2]_1$ and $3p^5\ (^2P_{3/2})nd\ [1/2]_0$ carry 100 and 50 respectively. Therefore, the assignments of the Rydberg series are straightforward. This consonant is further supplemented by the quantum defects at the lower n-values.

$$3p^5 4p'\ [1/2]_1 \rightarrow 3p^5\ (^2P_{3/2})\ nd\ [3/2]_1$$
$$nd\ [1/2]_{1,0}$$
$$3p^5 4p'\ [1/2]_1 \rightarrow 3p^5\ (^2P_{3/2})\ ns\ [3/2]_{1,2}$$

The $3p^5(^2P_{3/2})nd\ [3/2]_2$ series is the strongest of all the observed Rydberg series and have been observed up to $n = 45$. The other relatively weak series is $3p^5(^2P_{3/2})nd\ [1/2]_1$ that was the weakest series in the photoabsorption experiment (Yoshino 1970). The $3p^5(^2P_{3/2})nd\ [3/2]_2$ series is resolved from the $3p^5(^2P_{3/2})nd\ [1/2]_1$ series up to $n = 25$ after that they merge into one Rydberg series. The $3p^5(^2P_{3/2})ns[3/2]_2$ series is resolved from the $3p^5(^2P_{3/2})\ nd[1/2]_1$ series up to $n = 24$. It is interesting to note that there is a clear evidence of intensity variation in the $3p^5(^2P_{3/2})nd[3/2]_2$ Rydberg series from $n = 20$ to 35, the two series sweep across an intensity minimum around $n = 27$ and afterwards the $3p^5(^2P_{3/2})nd\ [3/2]_2$ series gains oscillator strength. This intensity variation has been observed in all the spectra observed from all the three different intermediate levels.

Considering the excitation from the $3p^5 4p'\ [3/2]_1$ intermediate level the calculations of Faust and McFarlane (1964) predicts the intensities 189 and 80 for the $3p^5(^2P_{3/2})nd\ [5/2]_2$ and $3p^5(^2P_{3/2})nd\ [3/2]_1$ series respectively. Indeed we have observed the following Rydberg series with reasonable intensities:

$$3p^5 4p'\ [3/2]_1 \rightarrow 3p^5\ (^2P_{3/2})\ nd\ [5/2]_2$$
$$3p^5\ (^2P_{3/2})\ nd\ [3/2]_1$$
$$\rightarrow 3p^5\ (^2P_{3/2})\ ns\ [3/2]_{1,2}$$

The situation gets even more simpler for the series attached to the $3p(^2P_{1/2})$ limit. Here, only one well defined autoionizing series of d-character have been detected in addition to the $3p^5\ (^2P_{1/2})ns\ [1/2]_{0,1}$ series.

From the third $3p^5 4p'\ [3/2]_2$ intermediate level the predicted intensities for the $3p^5\ (^2P_{3/2})nd\ [5/2]_3$ and $3p^5\ (^2P_{3/2})nd\ [3/2]_2$ series are 294 and 144 respectively. The following Rydberg series have been identified:

$$3p^5 4p'\ [3/2]_2 \rightarrow 3p^5\ (^2P_{3/2})\ nd\ [5/2]_3$$
$$3p^5\ (^2P_{3/2})\ nd\ [3/2]_2$$
$$\rightarrow 3p^5\ (^2P_{3/2})\ ns\ [3/2]_{1,2}$$

5. Spectrum of Krypton:

The ground state electronic configuration of krypton $4p^6\ ^1S_0$ and the ionic levels $5p^5\ (^2P_{3/2})$ and $4p^5\ (^2P_{1/2})$ serve as series limits at 112914.40 cm^{-1} and 118284.50 cm^{-1} respectively (Sugar and Musgrove 1991). The excitation of an electron from the 4p sub-shell yields four levels $4p^5 5s[3/2]_2$, $4p^5 5s[3/2]_1$, $4p^5 5s'[1/2]_0$, $4p^5 5s'[1/2]_1$. The levels $5s[3/2]_2$ and $5s'[1/2]_0$ are metastable while the $5s[3/2]_1$ and $5s'[1/2]_1$ combine with the lower state.

A single photon excitation from the ground state yields five dipole allowed Rydberg series. Three series namely $4p^5(^2P_{3/2})nd\ [1/2]_1$, $nd[3/2]_1$ and $ns[3/2]_1$ are attached to the first ionization threshold and two series are attached to the second ionization threshold, $4p^5(^2P_{1/2})nd\ [3/2]_1$ and $ns[1/2]_1$. In figure 5.2 we present the spectra covering the energy region between 568 – 553 nm showing the three lines excited by the first laser from the $4p^5 5s[3/2]_2$ metastable level. Since these levels have been used as intermediate levels to access the high Rydberg states in krypton it is therefore important to look at their relative intensities.

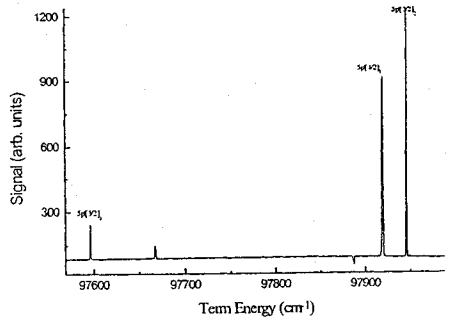

Figure 5.2 *Single photon Optogalvanic spectra of krypton showing the three intermediate levels excited from the metastable state* $4p^5(^2P_{3/2})5s[3/2]_2$.

Fig. 5.2

The $4p^5 5p'\ [3/2]_2$ and $4p^5 5p'\ [1/2]_1$ lines are dominant and $4p^5 5p'\ [3/2]_1$ is nearly 5 times lower in intensity as compared to the other two lines. Consequently, we have observed strong Rydberg series attached to the first ionization limit from the $4p^5 5p'\ [1/2]_1$ and $4p^5 5p'\ [3/2]_{12}$ levels whereas strong autoionizing Rydberg series have been observed converging to the second ionization limit from the $4p^5 5p'\ [3/2]_1$ level. The propensity rules for electric dipole transitions in the $j\ell K$-coupling scheme are: $\Delta\ell = \pm 1$; $\Delta j = 0$; $\Delta K = 0, \pm 1$ and $\Delta J = 0, \pm 1$. These rules are well behaved and wherever $\Delta K = \Delta J = +\Delta\ell$, the line possesses higher intensity. However, the $\Delta j = 0$ rule is not followed strictly since transitions with the change of the ionic core are also observed. Consequently, the Rydberg series built on $4p^5(^2P_{3/2})$ and $4p^5(^2P_{1/2})$ ionic levels have been observed with reasonable intensities. The following, relatively stronger, Rydberg series are expected from each of the intermediate level converging to the $4p^5(^2P_{3/2})$ and $4p^5\ (^2P_{1/2})$ limits:

(a) $4p^5(^2P_{1/2})5p[1/2]_1 \rightarrow 4p^5(^2P_{3/2})\ nd\ [3/2]_2$
$(^2P_{1/2})\ nd\ [3/2]_2$

(b) $4p^5(^2P_{1/2})5p[3/2]_1 \rightarrow 4p^5(^2P_{3/2})\ nd\ [5/2]_2$
$(^2P_{1/2})\ nd\ [5/2]_2$

(c) $4p^5(^2P_{1/2})5p[3/2]_2 \rightarrow 4p^5(^2P_{3/2})\ nd\ [5/2]_3$
$(^2P_{1/2})\ nd\ [5/2]_3$

The absolute term values (in cm^{-1}) are calculated by adding the excitation energy to the energy of the relevant intermediate level listed by Sugar and Musgrove (1991).

$2p^5 3p'\ [1/2]_1 = 97919.1400\ cm^{-1}$

$2p^5 3p'\ [3/2]_1 = 97595.9086\ cm^{-1}$

$2p^5 3p'\ [3/2]_2 = 97945.1597\ cm^{-1}$

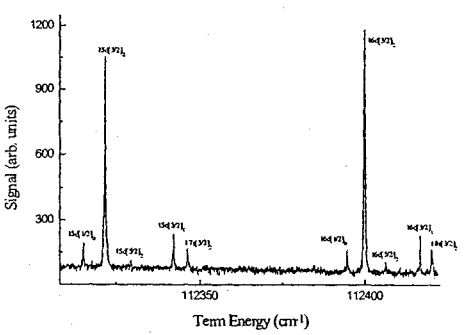

Figure 5.3a *Two step Optogalvanic spectra of krypton covering the spectral region between 112310 cm^{-1} to 112423 cm^{-1} excited from the $4p^5(^2P_{1/2})5p[1/2]_1$ level and converging to first ionization limit.*

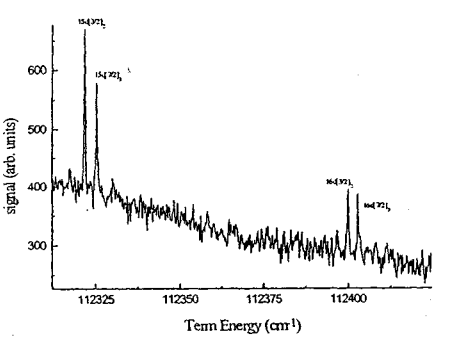

Figure 5.3b *Two step Optogalvanic spectra of krypton covering the spectral region between 112310 cm^{-1} to 112423 cm^{-1} excited from the $4p^5(^2P_{1/2})5p[3/2]_2$ level and converging to first ionization limit.*

Fig. 5.3

Figure 5.3a shows a small portion of the spectra covering the energy region between 112320 – 112420 cm^{-1} excited from the $4p^5 5p'\ [1/2]_1$ intermediate level. The dominating lines are $4p(^2P_{3/2})nd[3/2]_2$ (n = 15, 16) that follow $\Delta K = \Delta J = +\Delta\ell$ selection rules. The $4p(^2P_{3/2})nd[1/2]_0$ (n = 15, 16) are also present but remain very sharp and weaker as compared to the $4p(^2P_{3/2})nd[3/2]_1$ and $4p(^2P_{3/2})ns[3/2]_2$ lines. Although the $4p(^2P_{3/2})ns[3/2]_1$ are also expected but we have not observed these lines. In the photoabsorption experiment from the ground state the dominating lines are $4p(^2P_{3/2})nd[1/2]_1$, $4p(^2P_{3/2})nd[3/2]_1$ and $4p(^2P_{3/2})ns[3/2]_1$ (Yoshino and Tanaka 1979). In figure 5.3b we show the spectrum of krypton covering the same energy region as shown in figure 5.3a but excited from the $4p^5 5p'\ [3/2]_2$ intermediate level. The observed lines are identified as $4p(^2P_{3/2})nd[3/2]_2$ and $4p(^2P_{3/2})nd[7/2]_3$ (n = 15, 16). According to the propensity rules, the strongest series should be $4p(^2P_{3/2})nd[5/2]_3$ as observed in argon and neon but this series is absent in krypton.

Figure 5.4ab cover the energy region from 12500 to 112890 cm^{-1} showing the high members of the Rydberg series converging to the first ionization limit. The $4p(^2P_{3/2})nd[3/2]_2$ series have been observed up to n = 50 and the $4p(^2P_{3/2})ns[3/2]_2$ series up to n =37.

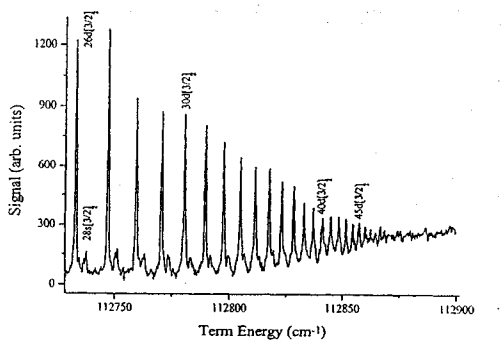

Figure 5.4 *Two step Optogalvanic spectra of krypton covering the spectral region between 112730 cm^{-1} to 112900 cm^{-1} excited from the $4p^5(^2P_{1/2})5p[3/2]_2$ level and converging to first ionization limit.*

6. The Spectrum of Xenon:

A schematic diagram of the excitation scheme in xenon is shown in figure 6.1.

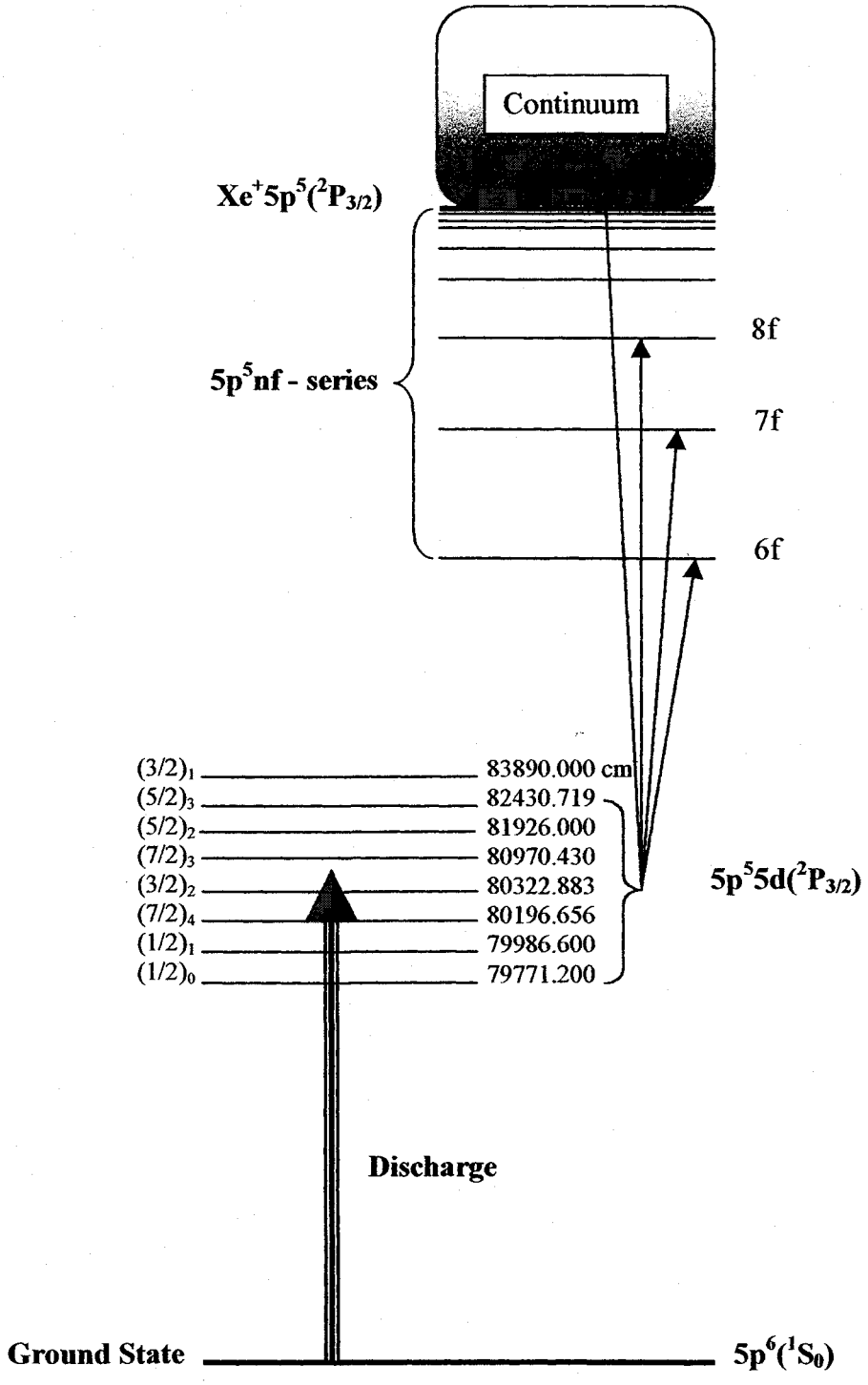

Fig. 6.1

The experiments were performed by filling xenon in the cell at a pressure of ~ 1 mbar. The discharge was initially ignited at about 400 volts through a ballast resistor of 70

kΩ. The voltage was slowly decreased to make the discharge operating in an electrically quiet mode. This condition was achieved at 180 volts and the current was ≅ 1mA whereas, the voltage noise amplitude was ≅ 0.5 mV. The optogalvanic signal was monitored through a coupling capacitor of 0.1 μF. The $5p^5 6s$ and $5p^5 5d$ configurations based levels of xenon were populated by running a mild discharge in the discharge cell. The levels based on the $5p^5 6s$ and $5p^5 5d$ configurations are strongly mixed in xenon which is shown to consists of 63% and 34% of these configurations respectively (Lieberman, 1971) and consequently, efficient excitation of the $5p^5 nf$ Rydberg levels from these levels are expected. We expect to see Rydberg series excited from each of these levels based on the $5p^5 5d$ configuration in the wavelength region between 500 – 730 nm. We have indeed observed all the expected $5p^5 nf$ J = 1 – 5 Rydberg series attached to the first ionization threshold.

Considering now the spectra observed in the wavelength region between 730 – 540 nm. The spectra in this region has been recorded using different dyes. The spectra show clear series limits that helped in arranging and assigning the levels to individual excitations. In this region, one expects to see at least eight series limits around 717 nm, 649 nm, 628 nm, 593 nm, 571 nm, 567 nm, 560 nm and 553 nm corresponding to $5p^5(^2P_{3/2})5d\ [3/2]_1$, $[5/2]_3$, $[5/2]_2$, $[7/2]_3$, $[3/2]_2$, $[7/2]_4$, $[1/2]_1$ and $[1/2]_0$ levels respectively. The relative intensities of the multiplets based on these excitations have been calculated by Faust and McFarlan (1964) within the framework of the jK-coupling scheme. In these calculations, the transition probability from a level belonging to the $5p^5(^2P_{3/2})$ parent ion to one belonging to the $5p^5(^2P_{1/2})$ parent ion is zero. The selection rules are: $\Delta j = 0$; $\Delta K = 0, \pm 1$ and $\Delta J = 0, \pm 1$. The calculations show that the strongest lines satisfy the selection rules: $\Delta K = \Delta J = +\Delta \ell$ and they occur for the highest J-values. The other relatively strong transitions follow the selection rules: $\Delta K = \Delta J = 0$ and $\Delta K = \Delta J = -\Delta \ell$ respectively.

Starting from the longest wavelength region, the lowest limit around 712 nm corresponding to excitation from the $5p^5 5d[3/2]_1$ level. The possible *nf*-Rydberg series alongwith their calculated relative intensities using jK-coupling scheme are:

$5p^5(^2P_{3/2})5d\ [3/2]_1$	→	$5p^5 nf\ [5/2]_2$	21166	$(\Delta K = \Delta J = +\Delta \ell)$
	→	$5p^5 nf\ [3/2]_1$	4410	$(\Delta K = \Delta J = 0)$

Although the region has been studied where these levels were expected but no transitions belonging to this excitation process were detected. The absence of the Rydberg series may be attributed to the fact that it is the highest lying level of the

$5p^5 5d$ configuration and it can decay quickly to the $5p^5 6p$ configuration based levels. As a result, the population of this level depletes and excitation from this level possess very low transition probabilities. The longest wavelength that is accessible with our laser system is about 730 nm. Therefore, the lowest members of the series that we can observe are $n = 9$ and 8 for the excitation from the $5d[5/2]_{2,3}$ levels and $n = 6$ for the rest of the excitation channels.

The possible excitation channels from the $5p^5 5d$ configuration based levels in the jK-coupling are presented below. The $5p^5 5d[5/2]_3$ excitation based series limit is expected around 649 nm and the possible nf Rydberg series are:

$5p^5(^2P_{3/2})5d\ [5/2]_3$	$\rightarrow$	$5p^5 nf\ [7/2]_4$	48600	$(\Delta K = \Delta J = +\Delta \ell)$
	$\rightarrow$	$5p^5 nf\ [5/2]_3$	10240	$(\Delta K = \Delta J = 0)$
	$\rightarrow$	$5p^5 nf\ [3/2]_2$	586	$(\Delta K = \Delta J = -\Delta \ell)$

The series limit around 628 nm corresponds to excitation from the $5p^5 5d[5/2]_2$ level and the possible nf Rydberg series are:

$5p^5(^2P_{3/2})5d\ [5/2]_2$	$\rightarrow$	$5p^5 nf\ [7/2]_3$	36000	$(\Delta K = \Delta J = +\Delta \ell)$
	$\rightarrow$	$5p^5 nf\ [5/2]_2$	7166	$(\Delta K = \Delta J = 0)$
	$\rightarrow$	$5p^5 nf\ [3/2]_1$	378	$(\Delta K = \Delta J = -\Delta \ell)$

The next series limit is expected around 593 nm corresponds to excitation from the $5p^5 5d[7/2]_3$ level and the possible nf Rydberg series are:

$5p^5(^2P_{3/2})5d\ [7/2]_3$	$\rightarrow$	$5p^5 nf\ [9/2]_4$	55125	$(\Delta K = \Delta J = +\Delta \ell)$
	$\rightarrow$	$5p^5 nf\ [7/2]_3$	6075	$(\Delta K = \Delta J = 0)$
	$\rightarrow$	$5p^5 nf\ [5/2]_3$	300	$(\Delta K = \Delta J = -\Delta \ell)$

The expected series limit around 571 nm corresponds to excitation from the $5p^5 5d[5/2]_3$ level and the possible nf Rydberg series are:

$5p^5(^2P_{3/2})5d\ [3/2]_2$	$\rightarrow$	$5p^5 nf\ [5/2]_3$	32928	$(\Delta K = \Delta J = +\Delta \ell)$
	$\rightarrow$	$5p^5 nf\ [3/2]_2$	7938	$(\Delta K = \Delta J = 0)$

The next series limit is expected around 567 nm corresponds to excitation from the $5p^5 5d[7/2]_4$ level. The possible nf Rydberg series are:

$5p^5(^2P_{3/2})5d\ [7/2]_4$	$\rightarrow$	$5p^5 nf\ [9/2]_5$	69300	$(\Delta K = \Delta J = +\Delta \ell)$
	$\rightarrow$	$5p^5 nf\ [7/2]_4$	7675	$(\Delta K = \Delta J = 0)$
	$\rightarrow$	$5p^5 nf\ [5/2]_3$	405	$(\Delta K = \Delta J = -\Delta \ell)$

The series limit around 560 nm corresponds to excitation from the $5p^5 5d[1/2]_1$ level and the possible nf Rydberg series are:

$5p^5(^2P_{3/2})5d\ [1/2]_1$	$\rightarrow$	$5p^5 nf\ [3/2]_2$	22050	$(\Delta K = \Delta J = +\Delta \ell)$
	$\rightarrow$	$5p^5 nf\ [3/2]_1$	4410	$(\Delta K = \Delta J = 0)$

The last series limit around 553 nm corresponds to excitation from the $5p^5 5d[1/2]_0$ level and the possible *nf* Rydberg series are:

$$5p^5(^2P_{3/2})5d\ [1/2]_0 \quad \rightarrow \quad 5p^5 nf\ [3/2]_1 \quad 8620 \qquad (\Delta K = \Delta J = +\Delta \ell)$$

Observing the same upper state from different intermediate levels serves as a check for the final J-value assignments. For example, the $5p^5 nf\ [3/2]_1$ Rydberg levels are observed from three intermediate levels: $5p^5 5d\ [1/2]_0$, $5p^5 5d[1/2]_1$ and $5p^5 5d[3/2]_1$ resulting in more reliable term energies for the upper levels. The $5p^5 nf\ [3/2]_2$ Rydberg series are observed from three intermediate levels: $5p^5 5d[1/2]_1$, $5p^5 5d[3/2]_2$ and $5p^5 5d[5/2]_3$ revealing consistent term energies within the quoted experimental error. Similarly, the $5p^5 nf\ [5/2]_3$ Rydberg series are observed from four intermediate levels: $5p^5 5d[3/2]_2$, $5p^5 5d[5/2]_3$, $5p^5 5d[7/2]_4$ and $5p^5 5d[7/2]_3$.

A portion of the spectrum covering the energy regions between 13760 – 13810 cm^{-1} is shown in the figure 6.2. The observed structure is identified as multiplets of the

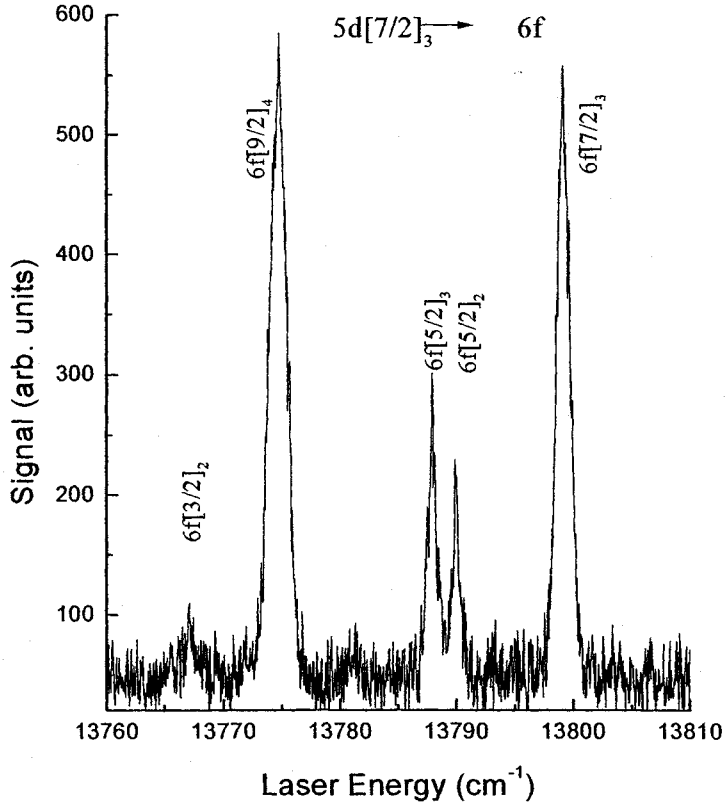

Figure 6.2 *A portion of the spectrum covering the region between 13760 cm^{-1} to 13810 cm^{-1} showing the prominent members of* $5d[7/2]_3 \rightarrow 6f$.

$5d[7/2]_3 \rightarrow 6f\,[3/2]_2$, $[9/2]_4$, $[5/2]_{3,2}$ and $[7/2]_3$ transitions respectively. The strongest line is $6f[9/2]_4$ and the other line with comparable intensity is $6f[7/2]_3$. The resolved doublet in the middle $6f[5/2]_{3,2}$ is nearly three times lower in intensity. The weakest transition correspond to $6f[3/2]_2$ level. The calculations of Faust and McFarlane (1964) predict the $6f[9/2]_4$ line nearly 9 and 200 times more intense as compared to the $6f[7/2]_3$ and $6f[5/2]_{2,3}$ lines respectively. Although the observed relative intensities do not match with the theoretical predictions but the trend is similar as predicted.

In figure 6.3 a-d the lowest multiplets as a result of excitation from the $5d[7/2]_4$, $[3/2]_2$, $[5/2]_2$ and $[5/2]_3$ levels respectively are presented. The group of lines belonging to the lowest observable member of the series from the $5d[7/2]_4$ levels is shown in figure 6.3a. In this excitation, the strongest line is $6f[9/2]_5$ and the other two lines are $6f[7/2]_4$ and $6f[5/2]_3$. Faust and McFarlane (1964) predicted the intensities of these

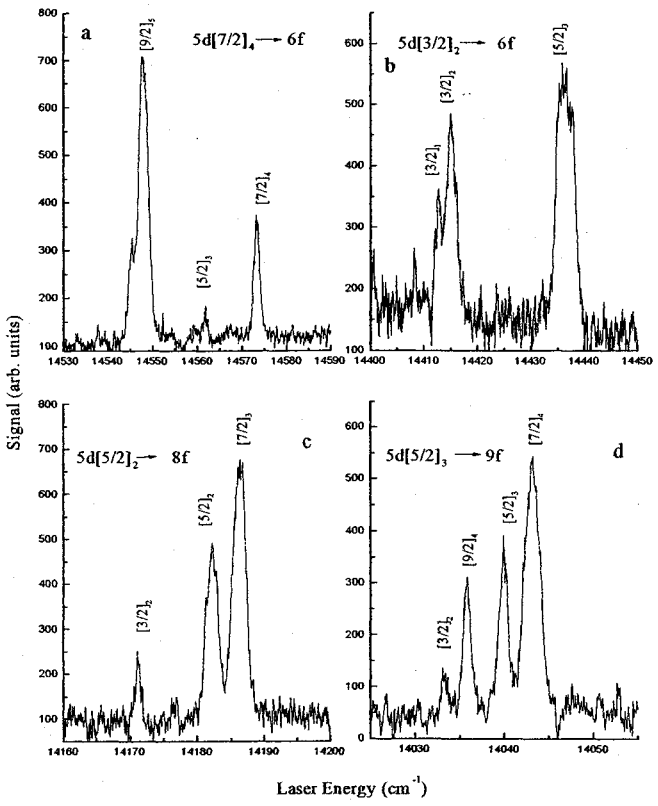

Figure 6.3 *Excitation spectra of xenon excited from (a) $5d[7/2]_4$, (b) $[3/2]_2$, (c) $[5/2]_2$ and (d) $[5/2]_3$ levels.*

lines as 69300, 7675 and 405 respectively. The multiplet structure of the lowest observable member of the series excited from the $5d[3/2]_2$ level are reproduced in figure 6.3b revealing $6f[3/2]_1$, $[3/2]_2$ and $[5/2]_3$ levels in order of increasing energy and intensity. The lowest series member observed in the excitation from the $5d[5/2]_2$ is shown in figure 6.3c. The calculated intensities are 32928 and 7938 for the $[5/2]_3$ and $[3/2]_2$ levels. The multiplet consists of transitions $5d[5/2]_2 \rightarrow 8f[3/2]_2$, $[5/2]_2$ and $[7/2]_3$ in order of increasing energy and intensity.The strongest line is $8f[7/2]_3$ and the weakest line is $8f[3/2]_2$. The calculations of Fraust and McFarlane (1964) predicts the $[7/2]_3$ component nearly 5 times intense as compared to the $[5/2]_2$ component. The group of lines in Fig. 6.3d around 14040 cm^{-1} are identified as multiplets $5d[5/2]_3 \rightarrow 9f$ $[3/2]_2$, $[9/2]_4$, $[5/2]_3$ and $[7/2]_{3,4}$ in order of increasing energy and intensity respectively. The predicted intensities of the multiplet components $[7/2]_4$, $[5/2]_3$ and $[3/2]_2$ are 48600, 10240 and 586 respectively. From the observed spectra it is clear that the strongest transitions obey the selection rules: $\Delta K = \Delta J = +\Delta\ell$ whereas, the other relative weaker transitions follow the selection rules: ($\Delta K = \Delta J = 0$) and ($\Delta K = \Delta J = -\Delta\ell$) respectively, in accordance to the theoretical calculations of Faust and McFarlane (1964).

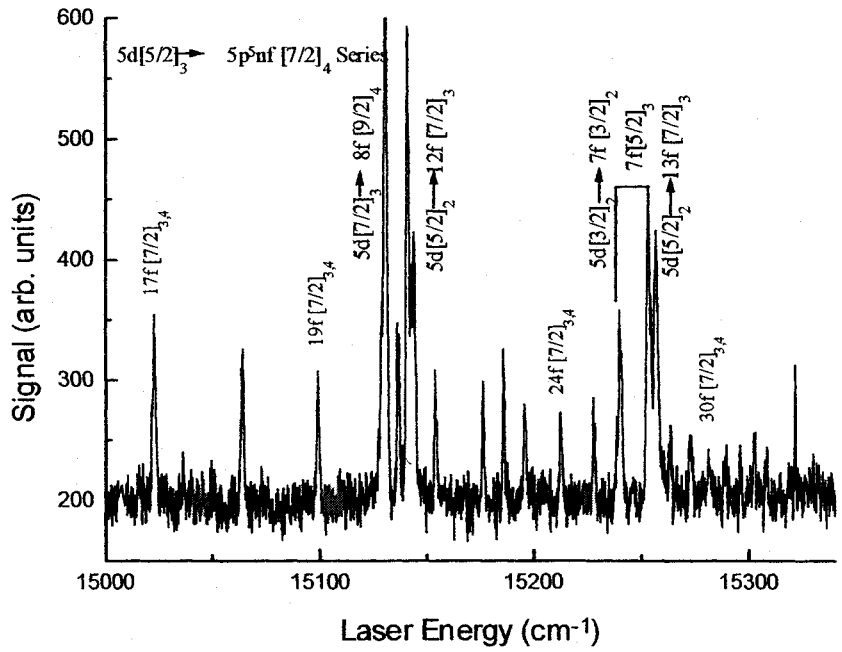

Figure 6.4a: *The optogalvanic spectra of xenon in the region between 15000 – 15350 cm^{-1} showing the $5d[5/2]_3 \rightarrow nf\,[7/2]_4$ Rydberg series. The stronger signals are identified as the lower members of the $5d[7/2]_3 \rightarrow 8f\,[9/2]_4, [7/2]_4$ and $5d[3/2]_2 \rightarrow 7f\,[3/2]_2\,[5/2]_2$ series.*

Figure 6.4 a-c show the Rydberg spectra excited from $5p^5 5d[5/2]_3$, $5p^5 5d[5/2]_2$ and $5p^5 5d[7/2]_3$ lower levels respectively. In figure 3.4a, the Rydberg series correspond to $5p^5 nf[7/2]_4$ ($17 \leq n \leq 35$) and the three very strong and well resolved lines around 15130 cm^{-1} that are identified as $5p^5 8f[7/2]_4$, $5p\ 8f[5/2]_{2,3}$ and $5p^5 8f[7/2]_{3,4}$ excited from the $5p^5 5d[7/2]_3$ level. In addition, the $5p^5 7f\ [7/2]_{3,2}$ and $[5/2]_3$ levels excited from $5p^5 5d[3/2]_2$ are observed around 15260 cm^{-1}. The two members of the $5p^5 nf\ [7/2]_4$ series (n = 12 - 13) excited from the $5p^5 5d[5/2]_2$ level are also present, whereas, the

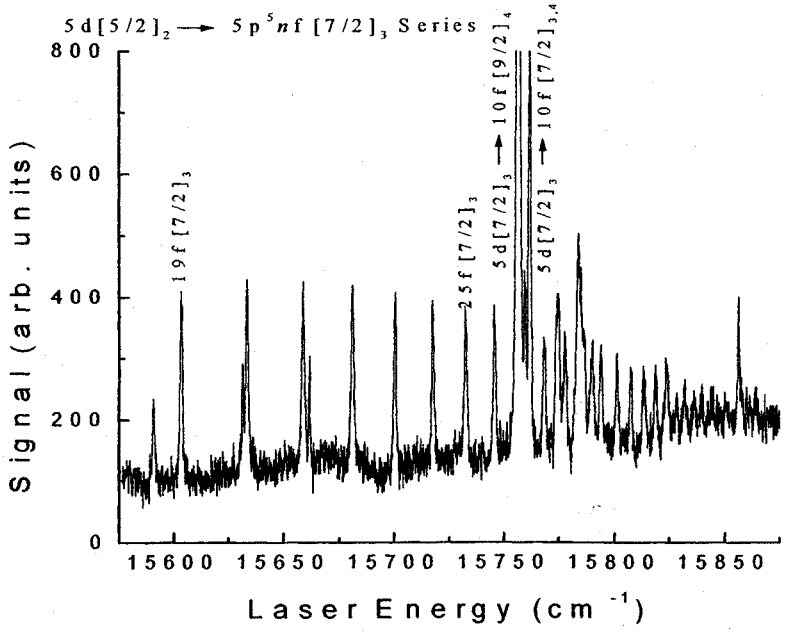

Figure6.4b: *The optogalvanic spectra of xenon in the region between 15575 – 15875 cm^{-1} showing the $5d[5/2]_2 \rightarrow nf\ [7/2]_3$ Rydberg series. The stronger signals are identified as $5d[7/2]_3 \rightarrow 10f\ [9/2]_4, [7/2]_4$.*

higher members of this series are shown in figure.3.4b. The dominating lines in figure. 6.4b are $5p^5 nf\ [7/2]_3$ ($19 \leq n \leq 40$) excited from the $5p^5 5d\ [5/2]_2$ lower level. The strong multiplet around 15760 cm^{-1} is identified as $5p^5 10f[9/2]_4$ and $5p^5 10f\ [7/2]_{3,4}$ excited from the $5p^5 5d[7/2]_3$ lower level.

Figure.6.4c shows the $5p^5 nf\ [9/2]_4$ Rydberg series ($20 \leq n \leq 40$) excited from the $5p^5 5d\ [7/2]_3$ lower level. A very strong line in the spectra around 16720 cm^{-1} is identified as $5p^5 11f\ [9/2]_5$ excited from the $5p^5 5d\ [7/2]_4$ lower level. A couple of other lines also appear which do not belong to the Rydberg series are identified as $5p^5 9f\ [3/2]_1$, at 16690 cm^{-1}, excited from the $5p^5 5d\ [1/2]_0$ level and around 16740 cm^{-1} as $5p^5 12f\ [5/2]_3$ excited from the $5p^5 5d\ [3/2]_2$ lower level.

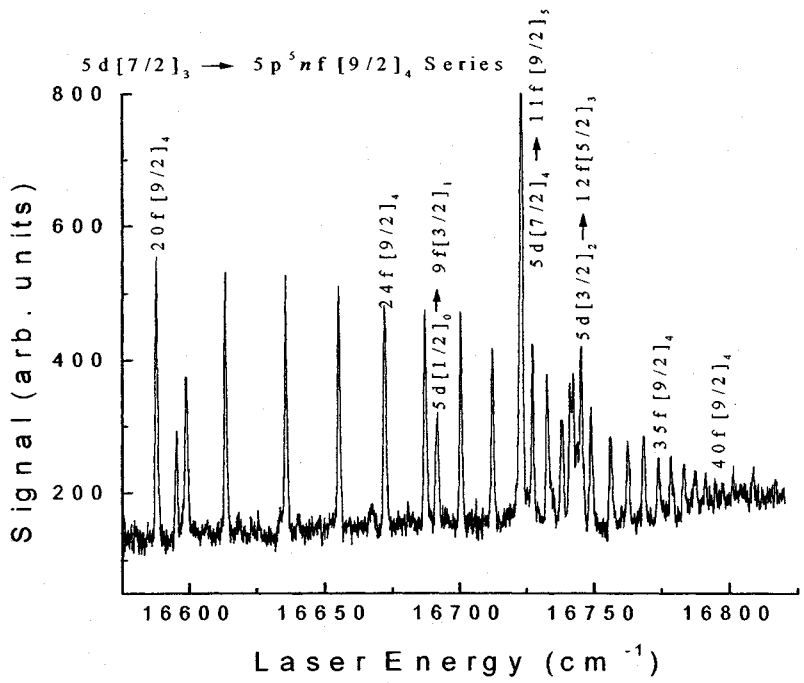

Figure 6.4c: *The optogalvanic spectra of xenon in the region between 16575 – 16825 cm^{-1} showing the $5d[7/2]_3 \rightarrow nf[9/2]_4$ Rydberg series. The stronger signals are identified as $5d[7/2]_4 \rightarrow 11f[9/2]_5$ and $5d[3/2]_2 \rightarrow 12f[5/2]_3$.*

In figures 6.5a,b the Rydberg series excited from the $5p^5 5d\ [7/2]_4$, $5p^5 5d\ [1/2]_1$, $5p^5 5d\ [1/2]_0$ and $5p^5 5d\ [3/2]_2$ lower levels are reproduced. In figure 3.5a, the dominating Rydberg series are $5p^5 nf\ [9/2]_5$ ($14 \leq n \leq 23$) and $5p^5 nf\ [5/2]_3$ ($16 \leq n \leq 35$) excited from the $5p^5 5d\ [7/2]_4$ and $5p^5 5d\ [3/2]_2$ lower levels respectively. An additional line at 17166 cm^{-1} is identified as $5p^5 5f\ [3/2]_1$ excited from the $5p^5 6s\ [1/2]_0$ lower level. At the lower energy side adjacent to $5p^5 18f\ [9/2]_5$ the peak is identified as $5p^5 13f\ [3/2]_1$ excited from the $5p^5 5d\ [1/2]_0$ level. Three members of the $5p^5 nf\ [3/2]_2$ series (n = 13 - 15) excited from the $5p^5 5d\ [1/2]_1$ lower level are also identified. In figure 3.5b, the Rydberg series terminating on to three limits are clearly discernible these correspond to $5p^5 nf\ [9/2]_5$ ($24 \leq n \leq 35$), $5p^5 nf\ [3/2]_2$ ($17 \leq n \leq 30$) and $5p^5 nf\ [3/2]_1$ ($14 \leq n \leq 18$) excited from the $5p^5 5d\ [7/2]_4$, $5p^5 5d\ [1/2]_1$ and $5p^5 5d\ [1/2]_0$ lower levels respectively. The intense doublet around 17550 cm^{-1} is attributed to $5p^5 6f\ [3/2]_{1,2}$ levels and the line at 17570 cm^{-1} is identified as $5p^5 6f\ [5/2]_2$ excited from the $5p^5 6s'\ [1/2]_1$ lower level.

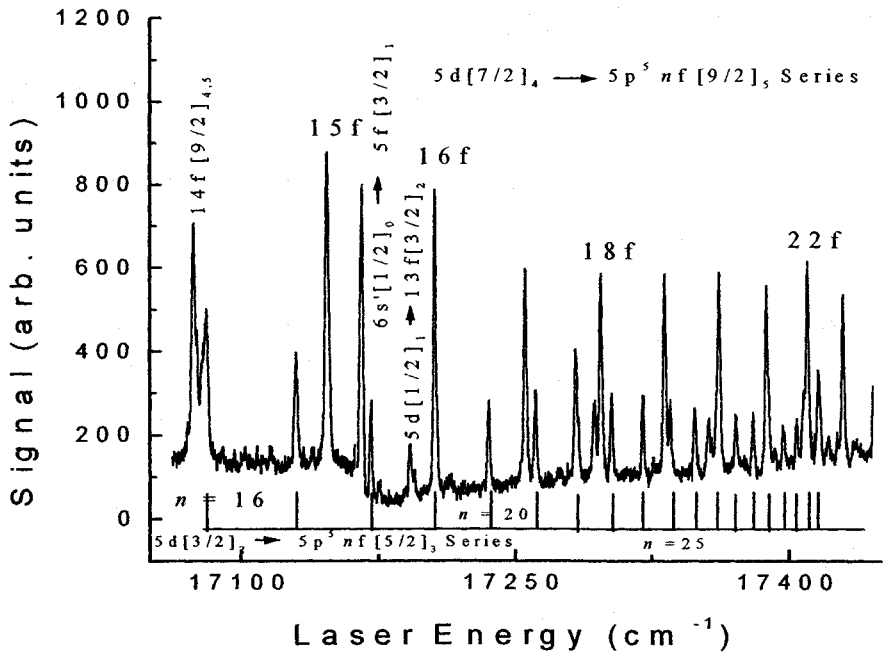

Figure 6.5a: *The optogalvanic spectra of xenon in the region between 17050 – 17450 cm^{-1} showing the 5d[7/2]$_4$ → nf [9/2]$_5$ and 5d[3/2]$_2$ → nf [5/2]$_3$ Rydberg series. The lowest member of the series are excited from the 6s[1/2]$_0$ metastable level is also marked.*

In all the inert gas spectra, the lower members of the series built on the mp^5(^{2}P$_{1/2}$) ionic level (m = 2, 3, 4 and 5 for neon, argon, krypton and xenon respectively) play an interesting role: below the first ionization threshold they interact with the series possessing the same K and J values resulting in series perturbations and above the first ionization threshold they decay into the p^5(^{2}P$_{3/2}$)$\varepsilon\ell$ adjacent continua and show Fano-type autoionizing resonance line shapes (Berkowitz 1979, Gallagher 1994, Connerade 1998). However, as far as the mp^5(^{2}P$_{1/2}$)*n*f-series is concerned, the situation is different in the spectra of xenon because the first member of the 5p^5*n*f series built on the 5p^5(^{2}P$_{1/2}$) ion core lies above the first ionization threshold. Consequently, all the 5p^5*n*f series converging to the first ionization threshold remain essentially unperturbed. However, a small perturbation may exist due to the interaction between the 5p^5(^{2}P$_{3/2}$) *n*f and the 5p^5(^{2}P$_{3/2}$) *n*p channels.

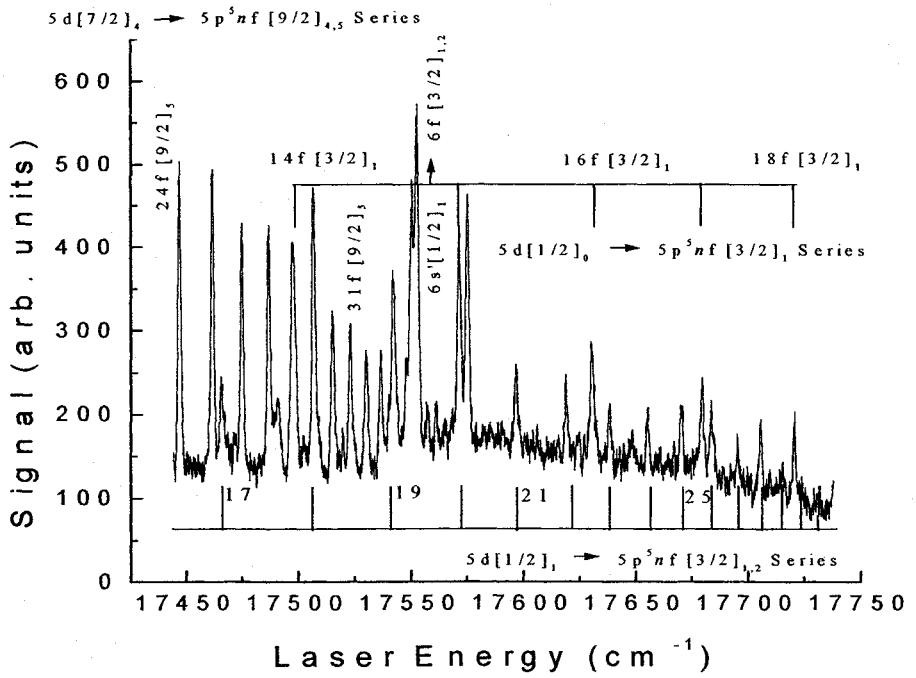

Figure 6.5b: *The optogalvanic spectra of xenon in the region between 17450 – 17750 cm^{-1} showing the higher members of the 5d[7/2]$_4$ → nf [9/2]$_5$ Rydberg series along with the 5d[1/2]$_0$ → nf [3/2]$_1$ and 5d[1/2]$_1$ → nf [3/2]$_2$ Rydberg series. The 6f[3/2]$_{1,2}$ and 6f[5/2]$_2$ multiplets excited from the 6s[1/2]$_1$ lower level are the dominating lines in this region*

The non-perturbed nature of all the Rydberg series suggests that a single channel quantum defect theory analysis will suffice the determination of ionization potentials relative to each of the intermediate levels. Each series was fit to the Rydberg relation:

$$En = IP - \frac{Ry}{(n-\mu_\ell)^2}$$

Where E_n is the measured energy of the Rydberg level, IP is the series limit, Ry is the mass corrected Rydberg constant 109736.856 cm^{-1} of xenon and μ is the quantum defect. Using an iterative technique, we have determined quantum defects and the convergence limits for the each series. Based on the listed values of the convergence limits and quantum defects, the differences between the observed and the calculated energies of the observed levels do not exceed 0.1 cm^{-1} in most of the cases. This shows that there is no systematic shift between the observed and the calculated energies which might exist due to Stark effects. An estimate of the net electric field present in the interaction region can be made from the combined Inglis-Teller and Holtzmark field expression (Ganguly 1986)

$$F = \frac{1.23 \times 10^9}{n_m^5}$$

where n_m is the principle quantum number whose intensity is equal to the background continuum signal and units of the electric field F are volts/cm. Whereas, the linear Stark splitting gives a lower limit of the electric field as:

$$F \geq \frac{0.857 \times 10^9}{n_m^5}$$

The stongest series detected in the present experimental setup has highest resolved n value of 60. This corresponds to n_m = 65, and the net electric field turns out to be about 1.06 volt/cm using the Inglis-Teller expression and 0.74 volt/cm using the linear Stark splitting relation. The linear Stark shift, using the hydrogenic approximation is given by White (1934):

$$\Delta E = 6.42 \times 10^{-5} n(n_2 - n_1)F$$

Here n_1 and n_2 are parabolic quantum numbers having values from 0 to $(n-1)$. The maximum value of the shift for n = 40 is 0.1 cm^{-1} which is well within the quoted experimental uncertainty in the energies. It may be mentioned that our Stark shift estimates is so low because we operated the discharge cell at a current much less than one mA.

Table

Rydberg series	Series limit	Quantum defect	Energy	H-P, 70	Diff.
$5d[1/2]_0 \rightarrow nf[3/2]_1$	18062.40 (8)	0.0524 (7)	79771.35	79771.76	+ 0.41
$5d[1/2]_1 \rightarrow nf[3/2]_2$	17847.20 (7)	0.0525 (8)	79986.55	79987.12	+ 0.57
$5d[3/2]_2 \rightarrow nf[5/2]_3$	17511.05 (7)	0.0291 (8)	80322.70	80323.24	+ 0.54
$5d[5/2]_2 \rightarrow nf[7/2]_3$	15908.25 (7)	0.0197 (8)	81925.50	81926.01	+ 0.51
$5d[5/2]_3 \rightarrow nf[7/2]_4$	15403.48 (7)	0.0183 (8)	82430.27	82430.70	+ 0.43
$5d[7/2]_3 \rightarrow nf[9/2]_4$	16863.30 (7)	0.0437 (8)	80970.45	80970.94	+ 0.54
$5d[7/2]_4 \rightarrow nf[9/2]_5$	17637.25 (8)	0.0353 (8)	80196.50	80197.13	+ 0.63
$6s[1/2]_0 \rightarrow nf[3/2]_1$	21637.00 (7)	0.0539 (6)	76196.75	76197.27	+ 0.52
$6s[1/2]_1 \rightarrow nf[3/2]_2$	20648.75 (7)	0.0524 (6)	77185.00	77185.54	+ 0.54

H-P,70 (Humphreys and Paul, 1970)

References

Ahmed M, Baig M.A. and Suleman B. 1997 *J.Phys.B*: **31** 4017

Ahmed M, Zia MA, Baig M.A. and Suleman B. 1997 *J.Phys.B*: **30** 2165

Aslam M, Ali Raheel, Nadeem A, Bhatti B A and Baig M A, 1999 *Opt. Commun.* **172**,37

Baig M.A, Connerade J.P and Pantelouris M. 1981 *Eur. Conf. Atomic Phys.* **5-A**, 109

Barbieri B and Beverini N 1990, *Rev. Mod. Phys.* **62**, 603

Berkowitz J. 1979 *Photoabsorption, Photoionisation and Photoelectron Spectroscopy*, Academic Press, New York.

Blazewicz P.R., Stockdale J.A.D, Miller J.C, Efthimiopoulos T and Fotakis C. 1987 *Phys. Rev. A* **35**, 1092

Bonin K.D, McIlrath T, and Yoshino K. 1985 *J.Opt. Soc. Am. B***2** , 1275

Cowan R.D, 1981 *The Theory of Atomic Structure and Spectra* (Uni. of California Press)

Demtröder W, 1998 *Laser Spectroscopy* (Springer-Verlag)

Gallagher T.F, 1994 *Rydberg Atoms* (Cambridge University Press)

Ganguly B N, 1986, *J. App. Phys.* **60**, 571

Gisselbrecht M., Marquette A. and Meyer M. 1997 *J.Phys.B*:, **31**, L977

Grandin J-P and Husson X. 1981 *J.Phys.B*: **14** , 433

Higgins M.J. and Latimer C.J 1993 *Phys. Scripts* **48**, 675

Humphreys C.J. and Paul E. 1970 *J.Opt. Soc. Am*, **60**, 1302

Kau R., Klar D., Schol S., Baier S. and Hotop H. 1996 *Z.Phys.D*: **36**, 23

King R.F and Latimer C.J 1982 *J.Opt. Soc. Am.* **72**, 306

Koeckhoven S.M, Buma W.J and de Lange C.A, 1994 *Phys. Rev. A* **49** , 3322

Koeckhoven S.M, Buma W.J and de Lange C.A 1995 *Phys. Rev. A* **51** ,1097

Knight R. D. 1986 *Phys. Rev. A***34**, 3809

Knight R. D. and Wang L.1985 *Phys. Rev. A***32**, 896

Knight R.D. 1985 *J.Opt. Soc. Am. B***2**, 1084

Knight R.D. and Wang L. 1986 *J.Opt. Soc. Am. B***3** , 1673

Labastie P, Biraben F and Giacobino E, 1982 *J.Phys. B*: **15**, 2595

Landais J, Huet M, Kucal H and Dohnalik T, 1995 *J.Phys. B*: **28**, 2395

Lemoigne J.P, Grandin J-P, Husson X and Kucal H 1984 *J.Physikque* **45**, 249

Letokhov S.V, 1987 *Laser Photoionization Spectroscopy* (Orlando)

L'Huillier A.L, Lompre L.A, Normand D, Morellec J, Ferray M, Lavancier J, Mainfray G. and Manus C. 1989 *J.Opt. Soc. Am. B***6** , 1644

Liberman S, 1969 J. Physique **30**, 53

Maeda K, Ueda K, and Ito K, 1993 *J.Phys.B*: **26** , 1541

Moore CE 1958 *Atomic Energy Levels* Vol **3**, NBS Circular 467, (Washington DC USA Govt. Printing Office)

Piracha, NK, Suleman, B, Khan SH and Baig MA 1995 *J.Phys. B*: **28**, 2525

Piracha, NK, Baig MA, Khan SH and Suleman, B 1997 *J.Phys. B*: **30**, 1151

Pratt S.T, Dehmer P.M and Dehmer J.L. 1987 *Phys. Rev. A***35**, 3793

Racah,G 1942 *Phys. Rev.* **62**, 438

Rundel R.D.,. Dunning F.B,. Goldwire H.C and. Stebbings R.F, 1975 *J.Opt. Soc. Am.* **72**, 628

Stebbings R.F, Latimer C.L, West W.P, Dunning F.B and Cook T.B 1975 *Phys. Rev. A***12**, 1453

Yoshino K. and. Freeman D.E 1985 *J.Opt. Soc. Am. B***2**, 1268

White H E, 1934, *Introduction to Atomic Spectra,* McGraw-Hill Company.